MECHANIKA
CZASOPISMO TECHNICZNE
TECHNICAL TRANSACTIONS
MECHANICS
WYDAWNICTWO POLITECHNIKI KRAKOWSKIEJ
4-M/2011
ZESZYT 7
ROK 108
ISSUE 7
YEAR 108

STANISŁAW ŁOPATA, PAWEŁ OCŁOŃ*

THE STRESS STATE ANALYSIS OF THE HIGH PERFORMANCE HEAT EXCHANGER

ANALIZA STANU WYTĘŻENIA WYSOKOSPRAWNEGO WYMIENNIKA CIEPŁA

Abstract

The paper presents the analysis of the stress state in the construction of the high performance heat exchanger with finned elliptical tubes. The thermal computations carried out using the control volume method are introduced and explained. The zones in the construction where the failure is the most probable are presented.

Keywords: *high performance heat exchanger, stress state*

Streszczenie

W artykule przedstawiono metodykę oceny stanu wytężenia konstrukcji wysokosprawnego wymiennika ciepła z ożebrowanymi rurami eliptycznymi. Omówiono sposób obliczeń cieplnych z użyciem metody objętości skończonych oraz wskazano miejsca konstrukcji wysokosprawnego wymiennika ciepła, w których prawdopodobieństwo pęknięcia rurek na skutek przekroczenia naprężeń dopuszczalnych jest największe.

Słowa kluczowe: *wysokosprawny wymiennik ciepła, wytężenie konstrukcji*

* Dr hab. inż. Stanisław Łopata, prof. PK, mgr inż. Paweł Ocłoń, doktorant, Katedra Maszyn i Urządzeń Energetycznych, Wydział Mechaniczny, Politechnika Krakowska.

Nomenclature

$\dot{m}_{in}$ – mass flow rate of water [kg/s]
p_{op} – operating pressure of water [bar]
T_{in} – water temperature at the inlet [K]
T_{out} – water temperature at the outlet [K]
T_b – bulk temperature of water [K]
c_p – specific heat capacity of water [J/(kg K)]
ρ – density of water [kg/m^3]
$\dot{q}_v$ – volumetric heat source [W/m^3]
$\dot{q}_w$ – heat flux density [W/m^2]
A_b – heat transfer area [m^2]
A_e – the cross-sectional area of the tube [m^2]
$\dot{Q}$ – heat flow [W]
h – heat transfer coefficient of water [W/(m^2 K)]
Γ – length of the boundary [m]

1. Wstęp

High performance heat exchangers based on elliptical tubes are widely used in many industries: the petrochemical, the automotive, the heavy and many others. Their compact design makes them possible to use as easily installed elements of heating drying and cooling installation. Their biggest advantage is the large heat transfer area in a compact volume, what makes them extremely efficient in heat exchange processes.

However, the compact volume of the device may bring about the problems in distributing the flow inside the heat exchanger. When the uniform or nearly uniform flow distribution inside the tubes in not ensured the thermal conditions in tubes are different. This causes that the thermal loading inside the tubes differs significantly, what may lead to exceeding the allowable stress level of the material and consequently to the failure of the heat exchanger [1, 2].

In the past the one of such failures of the high performance heat exchanger with the elliptical tubes was investigated. The tube, which was broken during the failure of the high performance heat exchanger, is presented on Fig. 1.

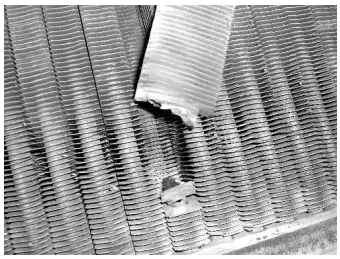

Fig. 1. The fractured tube of the high performance heat exchanger
Rys. 1. Uszkodzenie ożebrowanej rurki wysokosprawnego wymiennika ciepła

This damage of the tube is the effect of the excessive thermal loading inside the construction. The buckled bundle of tubes presented on a Fig. 2 confirms that the construction does not carry the thermal loads properly.

Fig. 2. The tube bundle in the high performance heat exchanger
Rys. 2. Widok wyboczonych rurek wysokosprawnego wymiennika ciepła

Aiming to analyze reasons of the failure necessary is to carry out the complex analysis that consists of flow distribution investigation, thermal and structural computation. The CFD analysis, which allows investigating the flow conditions inside the tubes, is carried out using the commercial code ANSYS CFX. The thermal computation, which permit to obtain the temperature distribution inside the tube are carried through with the usage of control volume method. Finally, knowing the temperature distribution inside the tubes, the structural analysis is undertaken to indicate the zones and locations of the construction, where the stress level exceeds the allowable values.

2. Design and operating conditions of the high performance heat exchanger

The high performance two-pass heat exchanger, which is the subject of investigation, is presented on a Fig. 3. The construction consists of two collectors and perforated bottoms, to which all the tubes are welded. The dense packed rectangular fins, assembled on the tubes surfaces, enhance the heat exchange area.

The gaseous medium (combustion gas) flows in perpendicular direction to the two rows of elliptical tubes exchanging its thermal energy with the water flowing inside the tubes. The upper collector is divided into two parts by the baffle. The water flows through the first half of tubes, turns round in the lower collector, and next coming through the second half of the tubes and the upper collector exits from the device through the outlet nozzle pipe.

The operating conditions of the investigated high performance heat exchanger are presented in a Table 1.

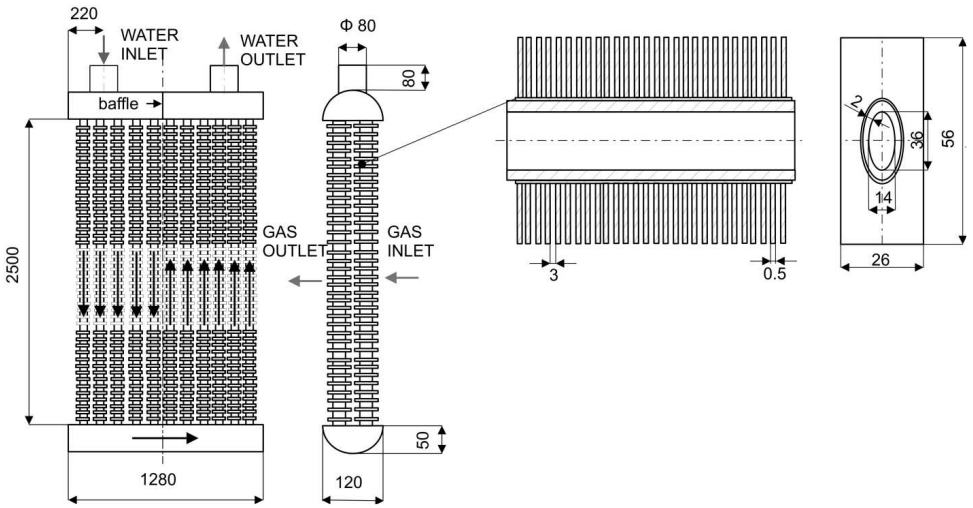

Fig. 3. The scheme of the high performance heat exchanger
Rys. 3. Schemat wysokosprawnego wymiennika ciepła

Table 1

The working parameters of the heat exchanger

Flow parameter	Value
$\dot{m}_{in}$ [kg/s]	22
p_{op} [bar]	6
T_{in} [K]	373
T_{out} [K]	< 403
$\dot{q}$ [W/m^2]	80 000

3. Analysis of the temperature distribution in elliptical tube

As mentioned before to carry out the structural analysis it is necessary to get to know the temperature distribution inside the elliptical tube. In the structural analysis, these temperatures are used as the thermal loads. However to obtain the temperature distribution inside the tube it is necessary to carry out the CFD analysis in order to obtain the boundary conditions for thermal analysis.

The computations of the bulk temperature T_b and the heat transfer coefficient h are carried out using CFD code ANSYS CFX. The results are presented on Fig. 4.

It is possible to observe on the figures above that the improper velocity distribution in the heat exchanger worsens significantly the heat transfer condition inside the whole device. The heat transfer coefficient in the first tubes of the second pass of the analyzed high performance heat exchanger is over six times lower than in the neighboring tubes. The reason of that is the very low liquid velocity inside these tubes. This result in liquid overheats, what confirms the bulk temperature values on Fig. 5 which exceed saturation temperature for 6 bar pressure (432 K).

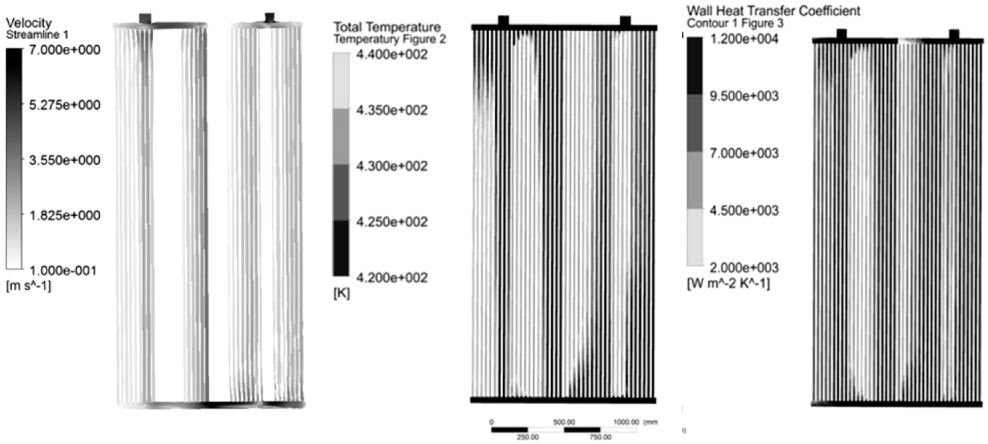

Fig. 4. Velocity distribution, bulk temperature distribution and the map of heat transfer coefficient
Rys. 4. Pole prędkości przepływu wody, rozkład temperatury wody i współczynnika wnikania ciepła w wymienniku ciepła

With the boundary condition from the CFD analysis, it is possible to carry out the thermal computation based on control volume method [3, 4]. The two-dimensional heat transfer problem is assumed, because of the largest thermal gradients along the thickness and the circumference of the tube. The heat conductance equation can be written in form:

$$c_p(T)\cdot\rho(T)\cdot\frac{\partial T}{\partial t} = -\mathrm{div}\dot{\mathbf{q}} + \dot{q}_v \tag{1}$$

Because the thermal steady-state is analyzed and in the domain do not exist any volume sources of heat, the dependence (1) can be simplified to the form:

$$\mathrm{div}\,\dot{\mathbf{q}} = 0 \tag{2}$$

Integrating equation (2) over the control volume *V*, the following equation for a single control volume (CV) is obtained:

$$-\int_V \mathrm{div}\,\dot{\mathbf{q}}\,dV = 0 \tag{3}$$

Applying the Gauss-Green-Ostrogradski theorem to eq. (3):

$$-\int_V \mathrm{div}\,\dot{\mathbf{q}}\,dV = -\int_S \mathbf{n}\cdot\dot{\mathbf{q}}\,dS \tag{4}$$

The equation (4) is written as a sum of heat flowing into the control volume through its boundary. The surface integral $-\int_S \mathbf{n}\cdot\dot{\mathbf{q}}\,dS$ is approximated summing the heat flow in from *k* neighboring cells:

$$-\int_S \mathbf{n}\cdot\dot{\mathbf{q}}dS = \sum_{i=1}^{k}\dot{Q}_i \tag{5}$$

The boundary conditions are being applied depending on its type. For the second type, when the constant heat flux density $\dot{q}_w$ and the heat transfer area $A_b = 1\cdot\Gamma = 1\cdot(\Gamma_a + \Gamma_b)$ of boundary are given, the equation (5) can be written in form:

$$-\int_S \mathbf{n}\cdot\dot{\mathbf{q}}dS = \sum_{i=1}^{l}\dot{Q}_i + \sum_{j=1}^{m}\dot{q}_w\cdot(\Gamma_j^a + \Gamma_j^b), \tag{6}$$

where:

m – is the number of boundary faces of the control volume,

l – is the number of non – boundary heat transfer surfaces.

For the third type boundary condition, when the constant heat transfer coefficient h, heat transfer area A_b and the fluid bulk temperature T_b are given the heat flowing into the cell can be written in the following form:

$$-\int_S \mathbf{n}\cdot\dot{\mathbf{q}}dS = \sum_{i=1}^{l}\dot{Q}_i + \sum_{j=1}^{m}h\cdot(\Gamma_j^a + \Gamma_j^b)\cdot(T_b - T) \tag{7}$$

On the Fig. 5 the control volume for two - dimensional case is presented.

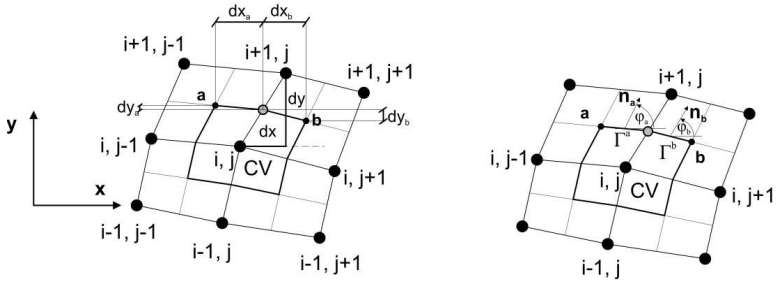

Fig. 5. Control volume

Rys. 5. Objętość kontrolna

With the assumption that the thermal conductivity λ is constant for the whole domain the heat balance equation (5) can be written according to formula:

$$\begin{aligned}(T_{i+1,j} - T_{i,j})\cdot S_{(i+1,j),(i,j)}(T_{i,j+1} - T_{i,j})\cdot S_{(i,j+1),(i,j)} + (T_{i,j-1} - T_{i,j})\cdot S_{(i,j-1),(i,j)} + \\ + (T_{i-1,j} - T_{i,j})\cdot S_{(i-1,j),(i,j)} = 0\end{aligned} \tag{8}$$

Where the boundary surface parameter $S_{(i+1,j)(i,j)}$ is obtained from the following dependency:

$$S_{(i+1,j),(i,j)} = \left(\frac{\cos\varphi_a\cdot\Gamma^a}{dy} + \frac{\sin\varphi_a\cdot\Gamma^a}{dx}\right)_{(i+1,j)(i,j)} + \left(\frac{\cos\varphi_b\cdot\Gamma^b}{dy} + \frac{\sin\varphi_b\cdot\Gamma^b}{dx}\right)_{(i+1,j)(i,j)} \tag{9}$$

After simplification the final dependence on $S_{(i+1,j)(i,j)}$ is:

$$S_{(i+1,\,j)(i,\,j)} = \left(\frac{dy_a}{dx} + \frac{dx_a}{dy} \right) + \left(\frac{dy_b}{dx} + \frac{dx_b}{dy} \right) \tag{10}$$

The analogical procedure is carried out to obtain the other surface parameters in equation (8).

The cross sectional area of the elliptical tube is divided into control volumes. The finite volume representation is presented on a Fig. 6.

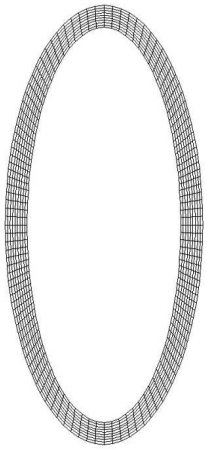

Fig. 6. Elliptical tube divided into control volumes
Rys. 6. Siatka numeryczna dla rurki eliptycznej

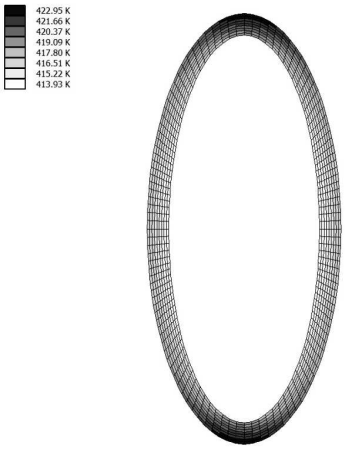

Fig. 7. Temperature distribution inside the elliptical tube
Rys. 7. Rozkład temperatury w rurce eliptycznej

For all CVs in the domain presented on Fig. 6 the heat balance equations (see eq. 8) are solved simultaneously, using the code written in c++ language. Next, the temperature distribution inside the elliptical tube is obtained. The tubes are divided into 500 segments along its length, as in CFD analysis. For each segment, the heat transfer coefficient h is averaged on the circumference based on the area of the control volumes faces. On the Fig. 7 as an example the temperature distribution for h = 4000 W/(m^2 K), T_b = 384 K and $\dot{q}$ = 80 000 W/m^2 is presented. Finally for all tubes the temperature distribution is obtained.

4. Structural analysis

As mentioned before, the thermal analysis was carried out in order to obtain the temperature distribution inside the tubes. Next, these temperatures are the thermal loads for the structural analysis.

The ANSYS Structural software is used in order to obtain the information about the displacements and stress distribution inside the construction. The element used for

analysis is 4-node shell element – SHELL 63. This finite element has six degrees of freedom in each node, the three translational and rotational. The mid – surface is its representation in a system. The maximal stress is calculated as the larger of the stresses on the outer and inner fibers of shell element.

In the structural analysis the thermal, pressure and gravity loads are taken into consideration.

On the Fig. 8 the displacement boundary conditions for static analysis are presented. This support ensures that all of the rigid body motions are constrained. The flat bars protect the tube bundle against the buckling. These bars are modeled as translational constraint acting in the direction perpendicular to the tubes.

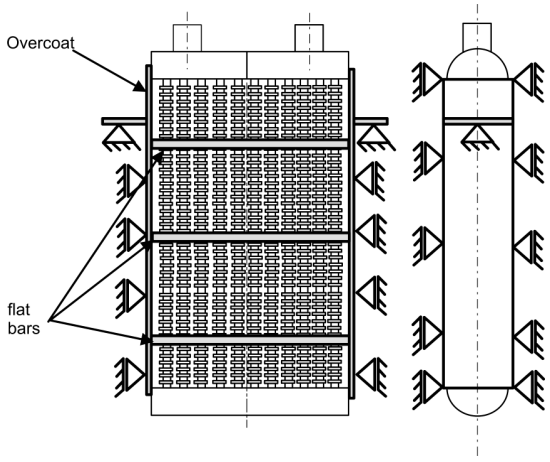

Fig. 8. The boundary condition for structural analysis
Rys. 8. Warunki brzegowe dla analizy wytrzymałościowej

Because the overcoat is not cooled its temperature is assumed equal to 603 K, slightly less than the temperature of combustion gas – 680 K. The temperatures of collectors and perforated bottoms are incorporated form the thermal analysis, which for bottoms and collectors is carried out in the assumption of one-dimensional heat conduction with the second type boundary condition for the value of $\dot{q}$ shown in the Table 1.

The main property of the SHELL 63 element is its thickness. In a Tab. 2 the thicknesses of the parts of the construction are presented.

Table 2

The thicknesses of components of the high performance heat exchanger

Part	Thickness [mm]
tube	2
overcoat	5
perforated bottom	18
collector	12

The material from which the construction in made is the Structural Steel-P355NH. It is assumed that the Young Modulus E equals 190 000 MPa for the mean temperature

of the construction = 450 K. The material density is assumed 7860 kg/m^3 and the Poisson ratio v equals 0.3. The guaranteed yield strength of material equals 360 MPa.

On a Fig. 9, the displacements of the construction are presented. It is possible to observe that the lower perforated bottom compresses the tubes in the second pass, especially the first two nearest the axis of symmetry of the device. The map of compressible stresses is presented on a Fig. 10. In the two aforementioned tubes the maximum compressible stress approaches 150 MPa.

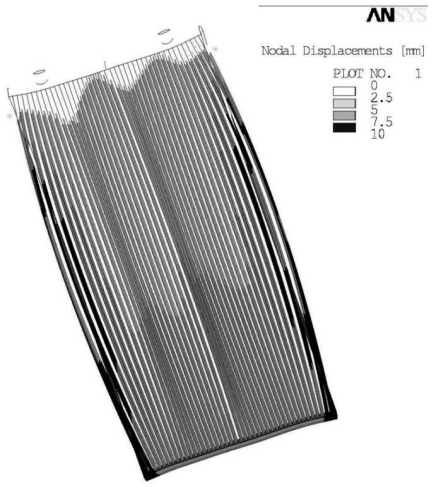

Fig. 9. The displacements of the elements of construction
Rys. 9. Przemieszczenia elementów konstrukcji

Fig. 10. The map of compressible stresses in the construction
Rys. 10. Mapa naprężeń ściskających dla konstrukcji

The tubes are long and thin therefore it is necessary to check if the available buckling load is not exceeded in this case. Therefore, the linear buckling analysis is carried out for a single tube, to obtain the available buckling load for the single tube.

On the Fig. 11 the tube subjected to the compressive force F_c = 1000 N is shown. For this model, the ANSYS Structural code computes the load multiplier, which answers how many times the allowable buckling load F_{ba} exceeds the $F_{c.}$

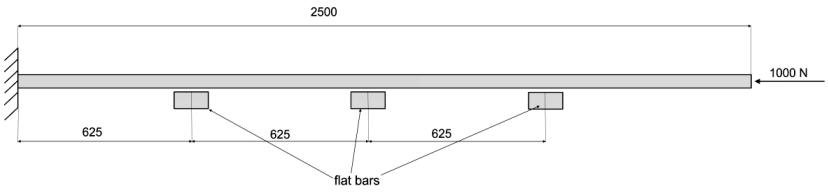

Fig. 11. The schematic model for buckling analysis
Rys. 11. Model przyjęty do analizy stateczności konstrukcji

The obtained value for the multiplier equals 8.6, therefore the allowable buckling load F_{ba} = 8600 N. The allowable buckling stress σ_{ba} obtained by dividing the F_{ba} by A_e equals

56 MPa. Therefore, inside the first two tubes, in the second pass in the first and the second row, the allowable buckling stress is exceeded. The tube break down is also probable for the tubes in the first pass slightly of the right from the inlet nozzle. For these tubes, the velocity is also low, decreasing the heat transfer conditions considerably and causing the excessive thermal loads acting on the tubes.

5. Conclusions

Presented structural analysis of the stress state in high performance heat exchanger shows that the improper flow distribution inside the device effects in excessive compressive loads acting on the tubes. This leads to the fracture of the tube due to exceeding allowable buckling loads and to the heat exchanger failure, what is possible to observe on Fig. 1 and 2.

The computational procedure described above can be useful in cases when it is necessary to access the stress state level in the construction of the high performance heat exchanger, or to indicate the zones where the failure is possible.

In order to the accuracy of the presented computation it is necessary to use SHELL 181 elements, which behaves more proper than SHELL 63 elements during the modeling of buckling state. Furthermore, it is necessary to investigate more precisely the connection between the perforated bottom and the tube using the submodeling techniques. These results will be presented in the future.

References

[1] Łopata S., Ocłoń P., *Investigation of the flow conditions in high performance heat exchanger*, Archives of Thermodynamics, Vol. 31, No. 3, Wydawnictwo IMP, Gdańsk 2010, 37-53.

[2] Ocłoń P., Łopata S., *Wpływ rozpływu cieczy na w wysokosprawnym wymienniku ciepła na jego warunki pracy*, praca zbiorowa pt. *Systemy, technologie i urządzenia energetyczne*, pod red. J. Taler, t. 2, Wydawnictwo Politechniki Krakowskiej, Kraków 2010.

[3] Taler J., Duda P., *Solving Direct and Inverse Heat Conduction Problems*, Springer, Berlin 2006.

[4] Chung T.J., *Computational Fluid Dynamics*, Cambridge Univ. Pres, 2002.